

High intensity specular reflectometry

first experiments

J. Stahn^a U. Filges^b T. Panzner^b

^aLaboratory for Neutron Scattering, and ^bLaboratory for Developments and Methods,
Paul Scherrer Institut, 5210 Villigen PSI, Switzerland

corresponding author: Jochen Stahn,
e-mail: jochen.stahn@psi.ch,
tel: +41 56 310 2518, fax: +41 56 310 2939

Abstract

Selene is the attempt to implement a new scheme for high-intensity specular reflectometry. Instead of a highly collimated beam one uses a convergent beam covering a large angular range. The angular resolution is then performed by a position-sensitive detector. Off-specular scattering in this set-up leads to some background, but for screening of wide parameter ranges (e.g. temperature, electric and magnetic fields) the intensity gain of at least one order of magnitude is essential. If necessary, the high precession measurements (even with off-specular components) then are performed with the conventional set-up. The heart of this new set-up is an elliptically focusing guide element of 2 m length. Though this guide is optimised for the use on the TOF reflectometer Amor at SINQ, it can be used as stand-alone device to check the possible application also for other neutron scattering techniques. The first measurements on AMOR confirmed the general concept and the various operation modes. A draw-back occurred due to problems with the internal alignment of the guide. Nevertheless in the TOF mode a gain factor of 10 was reached, and a factor 25 can be expected for an improved guide.

keywords: neutron, reflectometry, elliptic guide, focusing

1 the ideal

In a first step we developed an *ideal* neutron reflectometer, based on the convergent beam concept by Ott [1] to gain intensity for specular reflectometry on small samples. The idea to use half an elliptic guide for this purpose has already been published.[1, 2] But the idea of using elliptic guides is much older and has

been tested and realised several times in the past. [3, 4]

Besides this approach, there are other concepts on the market [5, 6] and under investigation [7] to skip the off-specular signal to decrease the measurement times for specular reflectometry.

1.1 principles

The design of the reflectometer study *selene* is based on the following principles:

- *The beam characteristics are defined at the sample.* This means that the expected sample size and the acceptable or intended divergence and wavelength range are identified, and that all components are optimised to operate within these ranges. A consequence is e.g. that the coating of a guide might be optimised for high reflectance instead of high reflecting angles.
- *Useless neutrons have to be avoided,* since they cause radiation and background problems. This is essentially true for the avoidable illumination of the sample environment, caused by a divergent beam. The smaller the sample the more one profits of using a focused beam.
- *Any beam filtering / shaping should be performed as early as possible.* Again this leads to lower background, reduces radiation problems, and the shielding design can be simplified. E.g. the fraction of neutrons finally arriving at the sample at a reflectometry set-up is of the order 10^{-4} compared to the intensity leaving a conventional straight guide. In this case the neutrons not used are absorbed or scattered within a few meters from the sample (and detector).
- *Optimisation vs. universality:* Every degree of freedom to have a more flexible instrument leads to some compromise. So often a multi-task instrument becomes quite complicated and does not allow for state of the art measurements. It

might be cheaper and more efficient to build several *simple* but highly specialised instruments.

In the present case the instrument is optimised for *specular reflectometry on small samples*. Where small means surface area in the range of some mm². For these samples it is very demanding and time-consuming to measure off-specular reflectivity and in most cases one is content to obtain specular reflectivity curves for a few external parameters, only. A screening of larger temperature or magnetic or electric field ranges is very time consuming.

To shorten the measurement time for specular reflectivity curves, at least for screening purposes, F. Ott suggested to use a beam converging to the sample and covering a large range of incidence angles.[1, 6] This concept, called REFocus, can be assessed as an angle dispersive reflectometer set-up, but with a strongly converging beam (the sample is in the focal point) with a relation between the angle of incidence on the sample α_i^s and the wavelength $\lambda = \lambda(\alpha_i^s)$. The focusing and λ selection is performed by one branch of an elliptically shaped guide element (acting as a lense) which is coated with a monochromatising multilayer (ML). The period of the ML might be graded along the guide. For specular conditions on the sample one has the exit angle $\alpha_f^s = \alpha_i^s$ and thus the normal neutron momentum transfer $q_z = 4\pi \sin \alpha_f^s / \lambda(\alpha_f^s)$. Figure 1 illustrates the situation on the sample. The function $\lambda(\alpha_f^s)$ is given by the shape of the guide element and its coating. The measured quantity $I(\alpha_f^s)$ can be converted into reflectivity $R(q_z)$. Since a broad α_i^s -range is active simultaneously, the α_i^s - and thus q_z -resolution is given by the spacial resolution and distance to the sample of a position-sensitive detector (PSD). Assuming a homogeneous intensity distribution over the α_i^s range, the intensity gain relative to a conventional set-up with small $\Delta\alpha_i^s$ is proportional to $\Delta\alpha_{i,\text{REFOCUS}}^s / \Delta\alpha_{i,\text{conventional}}^s$, which is > 10 .

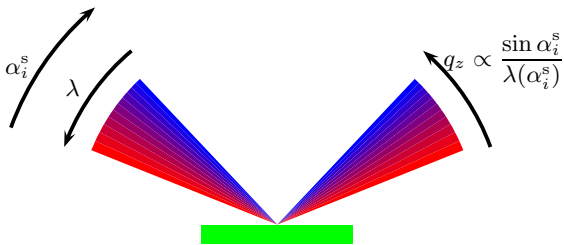


Figure 1: Principle of REFocus in the dispersive mode: an incoming convergent beam with a $\lambda(\alpha_i)$ encoding is specularly reflected off the sample (*green*). Since α_i and λ increase in the opposite direction, a large q_z range is covered simultaneously. In the case where α_i and λ increase in the same direction one has still dispersion, but at a much reduced range.

Depending on the orientation of the sample towards the incoming beam and the gradient of the ML-coating one has more or less dispersive geometries, depending on the needs of the experiment. F. Ott expects to cover a dynamic range of about 10^5 . The limitation is the off-specular scattering from the sample leading to a non-flat background.

REFocus fulfils the requirement for a convergent beam and thus a rather small illumination of the sample environment. But the monochromatisation is performed all along the guide and thus one has still a white beam close to the end of the guide.

1.2 selene concept

Based on REFocus we developed the selene concept to allow only those neutrons to enter the guide which are actually used at the sample. Since the ellipse ideally maps the pre-image (the virtual source) at one focal point to the adjoint one, this means that the beam should have the required properties already at the first focal point. This can be realised ...

(I) ...with a multilayer monochromator, where for each incident angle one has a different, but defined energy ($\lambda(\alpha_i)$ encoding): A ML-monochromator (reflecting at q_z^m) or a ML-bandpass is located directly in front of, or even at the first focal point. In combination with a small slit or knife-blade diaphragm it defines the virtual source to be mapped to the sample. The incoming divergent white beam is reflected from that monochromator if $4\pi \sin \alpha_i^m / \lambda \in \{q_z^m\}$. This means that for a given incoming-angle on the monochromator α_i^m a wavelength band according to the coating of the monochromator is reflected into α_f^m — which by the elliptic guide is transformed into an α_i^s at the sample. In the following this operation mode will be referred to as *monochromatic*.

(II) ...in time-of-flight (TOF) mode, where at a given time all neutrons have the same energy: Here the wavelength is encoded in $\lambda = \lambda(\text{TOF})$. As a consequence, optical errors of the monochromator or the elliptic guide (waviness, misalignment) do not influence the energy resolution, but just reduce the intensity on the sample.

(III) ...with a crystal monochromator, with a fixed and constant energy: This is conceptual the simplest approach, but in the present case the most difficult to realise. The geometry of the instrument would require crystals with a large mosaicity, and a double monochromator set-up.

This is because one wants to avoid moving the elliptic guide when changing the wavelength. This set-up will be investigated in the future.

Options I and II were tested and will be discussed in more detail. The actual λ -range is optimised due to the $I(\lambda)$ distribution of the source. In the sample plane the resolution conditions are relaxed and focusing is also favourable. But here the sample is no longer *point-like*, so it is more difficult to avoid over-illumination.

For small samples the virtual source does not have to be much larger than the projected height of the sample, i.e. it is in the sub-mm range — independent of the size of the complete guide. In the extreme case this means that a guide for a reflectometer needs an incoming aperture close to the source of some mm only, instead of the 30 to 50 mm used in conventional guides.

If off-specular measurements are required, or if the sample does not allow for using a large $\Delta\alpha_f$, it is possible to return to a configuration very close to the conventional angle-dispersive set-up. By reducing the divergence (and thus the λ -range) by a slit one gets a close-to-monochromatic beam and a high angular resolution. The intensity will be still slightly higher than in the conventional geometry due to less reflections in the guide. And the beam on the sample is still convergent and does not over-illuminate the sample more than necessary.

1.3 aberration and correction

Focusing guides show aberration effects. In case of an elliptic guide it is coma aberration, i.e. an off-axis point of the pre-image is projected onto a line in the image plane. The amount and direction of the distortion depends on where along the ellipse the reflection occurs. Figure 2 displays this effect.

The consequence is that (I) the size of the spot in the image plane is larger than the pre-image (the slit), defined by reflection in the early part of the guide; and (II) the size of the spot with a constant intensity for all incoming angles is smaller than the pre-image. This is caused by the focusing effect of reflections close to the end of the guide. For typical elliptic guides and sample sizes it turned out that due to the coma aberration the virtual source size has to be about 3 times the sample size. Then the complete sample is illuminated with the same divergence. The beam spot at the sample is then about 10 times the sample size, but the intensity drops fast outside the inner homogeneous region. One can estimate that about 30% of the beam hits the sample, the rest leads to illumination of the sample environment.

While this is already much less than compared to the usage of a divergent beam, it still leads to background problems. It is possible to correct for the

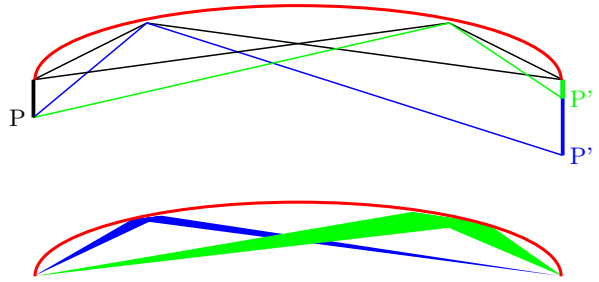


Figure 2: Sketches to illustrate coma aberration. *Top:* A beam from an off-axis point P of the pre-image is reflected off the reflector with an angular offset with respect to the ideal beam (from the focal point). This angular offset varies along the reflector: in the early part (*blue*) it is large, in the late part (*green*) it is small. As a result the reflected beams hit the second focal plane at various points P', the image is blurred. *Bottom:* On the other hand side beams from the first focal point emitted in a defined solid angle are reflected by a short / long part of the reflector in its early / late (*blue* / *green*) part. The result is that the beam is focused / de-focused. The combination of both effects leads to a distortion of the phase space, where its density stays constant.

coma aberration by dividing the guide into two identical elliptic parts which have one focal point in common. The coma aberration of the first guide leads to a blurred intermediate image in the joining focal plane. Due to the reversibility of the optical paths, this image is converted back to a sharp image at the sample position. Neglecting the limited reflectivity of the guides, one gets a beam at the sample position with almost the size given by a slit at the first focal point and the divergence defined by the acceptance of the elliptic guide.

P. Böni suggested to use subsequent elliptic guides, joining a focal point to allow for small beam-shaping elements like choppers and RF-coils.[8] In the cases with an even number of ellipses, coma aberration is no problem.

1.4 castle in the air

Disregarding real constraints like the finite width of radiation shielding and the non-perfect SM coating one can put together the items mentioned above to build an ideal reflectometer for small samples.

In detail, along the beam path: The early filtering means that a monochromator or chopper is placed directly behind the neutron source (in a way that a large divergence is collected). A very small first slit (opening exactly the projected height of the sample) forms the 1st focal point of first elliptic reflector. In

the 2nd focal point the beam can be manipulated further, e.g. it can be polarised or a 2nd chopper can be installed. Here the image is distorted by coma aberration, and (if relevant) the $\lambda(\alpha_i)$ encoding is not linear. A 2nd elliptic reflector with the same parameters as the first follows. Both reflectors share the 2nd focal point. The sample will be positioned in the 3rd focal point. Here aberration effects are almost cancelled and a quasi-linear $\lambda(\alpha_i)$ encoding is restored. A high-resolution (< 0.5 mm) PSD is positioned about 500 mm behind the sample.

2 the reality

The limited amount of resources and the absence of access to a free and freely configurable beam-port at a could source tell, that it is not realistic to test the instrument concept mentioned above by just building it. Instead we decided to build a down-scaled simplified version to be tested on the TOF reflectometer Amor at SINQ, PSI. Amor consists of an optical bench on which all components can be positioned with rather high flexibility. In short, the "cold source" is replaced by the end of the neutron guide; the ML-monochromator is positioned as close as possible to the end of the guide; a 2 m long elliptically shaped deflector is positioned in between monochromator and sample; and the detection is performed by the PSD.

This set-up restricts the available divergence to $\approx 1.2^\circ$ in the monochromatic mode and to $\approx 1.6^\circ$ for the TOF mode, respectively. Coma aberration is not corrected for. Nevertheless, it is possible to measure the gain factors for specular reflectivity; the fall-back option to the off-specular angle dispersive mode; and the problems caused by diffuse scattering from the monochromator.

2.1 experimental environment: Amor

Amor is a neutron reflectometer which allows for a wide range of set-ups.[9] The scattering geometry is vertical so that liquid surfaces are accessible. Most components are positioned on an optical bench which allows to play with the resolution, or to test exotic set-ups like the prism approach by R. Cubitt [7] or the selene concept. In general Amor is operated in TOF mode (realised by a double chopper), but it is also possible to run it with a monochromator.

For the tests presented here, the elliptic guide is positioned on the sample table (which allows for all necessary degrees of freedom) and the sample is on the analyser stage. The only restriction resulting from this shift is that the sample environment has to be small and light. The ML-monochromator is placed on the polariser stage and can be driven out of the beam to allow for using selene in TOF mode.

In the following sections the components are discussed in detail. The following conventions have been used: The laboratory coordinate system is right handed with x -axis horizontally along the beam, and z -axis vertical. Local coordinate systems follow this convention as much as possible. E.g. at the sample z is normal to the surface and x in the surface; both tilted to the laboratory system by only a few degrees. y is unchanged. For defining the various angles (relative to the lab system, the local system and eventually including deviations) a reference beam is introduced. It leaves the neutron guide at mid-height horizontally (x -direction). After that it is assumed to be specularly reflected in the xz -plane at all optical surfaces, i.e. by the double monochromator by $2\theta^m$ and $-2\theta^m$; by the centre of the elliptic guide by $2\theta^e$; and on the sample by $2\theta^s$. θ denotes the angle between the (reflecting) surface and the incoming reference beam, whereas α is the angle of some beam relative to the surface. The superscripts mean monochromator, elliptic guide, sample, and detector.

2.2 chopper

The chopper is positioned in a housing, some cm behind the end of the neutron guide. It consists of 2 discs, 490 mm apart, each with 2 openings of 13.6° . In general it is operated in a way to give $\Delta\lambda/\lambda = \text{const.}$ [10]

The chopper housing limits the maximum incoming divergence because it leads to a minimum distance between the end of the guide to the first diaphragm of 1500 mm. And to the first place where a monochromator can be installed (on the frame overlap filter stage) it is some 1800 mm.

For the tests we used a pulse frequency of 23.3 Hz (corresponding to 700 rpm).

2.3 multilayer monochromator

The monochromator is designed for a fixed geometry. The coating is a Ni/Ti bandpass with a plateau in the range $q_z^m \in [0.1 \text{ \AA}^{-1}, 0.11 \text{ \AA}^{-1}]$. This corresponds to $m \in [4.5, 5.0]$.

Two glass substrates coated with the mentioned ML are arranged face to face with a 3 mm gap to form a double monochromator. The glasses are shifted so that they just do not overlap (see figure 3). A knife blade atop the middle of the 2nd mirror is used to define the width of the beam in the 1st focal point of the ellipse.

The double monochromator was positioned on the polariser stage, 2744 mm after the end of the guide. Thus the maximum divergence to be expected there is $\Delta\alpha_i^m = 1.05^\circ$. This is the set-up shown in figure 8.

For this incoming divergence one gets a reflected beam with $\lambda \in [4.2 \text{ \AA}, 7 \text{ \AA}]$, and $\Delta\lambda/\lambda \approx 9\%$, only for $\lambda < 4.4 \text{ \AA}$ the resolution gets better due to cut

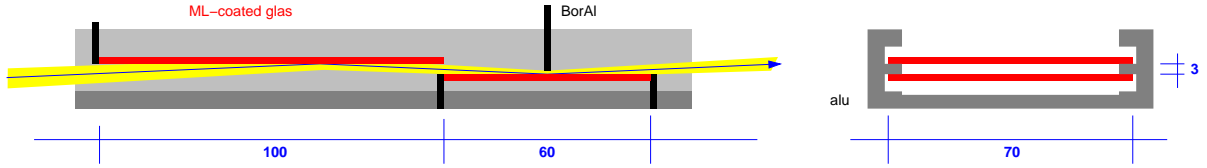


Figure 3: Cuts along (*left*) and normal (*right*) to the beam path through the double ML-monochromator. *Red* means glass substrate, *black* is the BorAl absorber and *yellow* the beam (coming from the left side).

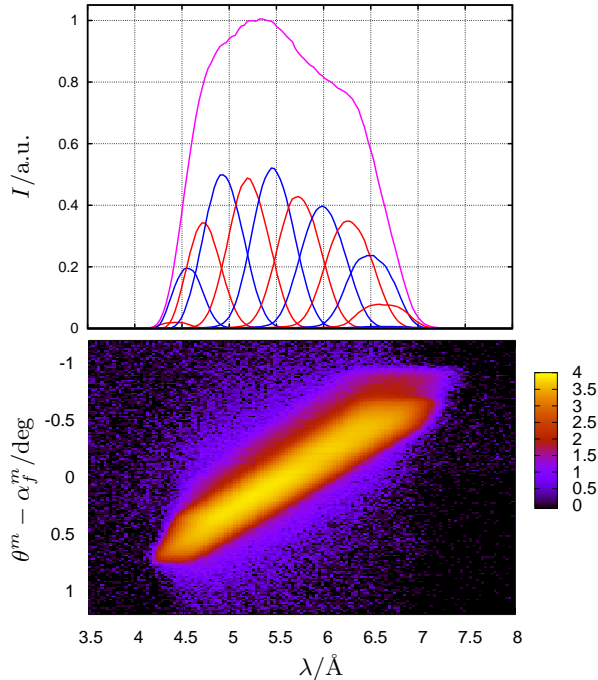


Figure 4: *Bottom*: Intensity map for $\theta^m = 3^\circ$ and $\Delta\alpha_i^m \approx 1.4^\circ$ on a logarithmic scale. $\log_{10} I(\lambda, \alpha_f^m)$ *Top*: Various cuts through that map along λ (*alternating red and blue*), and the total intensity as function of λ , integrated over α_f^m (*magenta*).

off effects, as can be seen in figure 4. This resolution still contains the $\Delta\lambda/\lambda \approx 4\%$ given by the chopper settings.

The intensity distribution for various α_f^m shown in figure 4, top, originates from the $I(\lambda)$ of the incident beam and for smaller λ (i.e. smaller α_i^m) also from the limited length of the monochromator.

Using this set-up with a monochromating ML offers the opportunity to switch easily to polarised neutrons by just replacing the ML by a polarising coating.[11]

2.4 elliptic guide

The guide has two functions: it has to focus the beam in the sample (xy) plane to the sample without taking care for the divergence; and it has to map the pre-image to the sample in the scattering (xz) plane, keeping a precise α_i/λ correlation.

The first aim is accomplished by the elliptic shape of the side-walls of the guide, where the second focal point is on the sample, while the first focal point is before the pre-image. The reason for this is that in the y -direction the sample is not really small with respect to the guide dimensions. Typical sample widths are 2 to 10 mm. Taking aberration into account this would mean a pre-image width of up to 30 mm — which is more than half of the length of short axis of the ellipse. The half axes parameters are $a_{xy} = 2025$ mm and $b_{xy} = 45$ mm. The side walls are coated with a Ni/Ti supermirror of $m = 3.5$.

The second aim is more demanding. The sample size in the scattering plane is given by the projection of the sample length normal to the incoming beam. This results in < 0.7 mm ($\alpha_i^s < 4^\circ$, sample length 10 mm). So pre-image and sample position define the foci of the elliptic shape of the reflector. The spacial constraints on Amor lead to a focus-to-focus distance of approximately 4000 mm. The half axes parameters are $a_{xz} = 2000$ mm and $b_{xz} = 50$ mm. The actual length of the device is given by the tolerable reflection angle for short wavelengths and the divergence to be collected. The *short wavelength* limit was defined to be 4 Å, which is at the flux maximum of the wavelength distribution behind the straight guide. And the maximum divergence delivered by the guide to a position behind the chopper shielding is $\Delta\alpha_i \approx 1.6^\circ$. Simulations and analytical calculations both showed an optimum length of 2000 mm, where the distances from the guide ends to both foci are 1000 mm. The complete length is coated with a Ni/Ti supermirror of $m = 5$. A sketch of the guide geometry is shown in figure 5.

The design of the elliptic guide element was done analytically and refined by McStas simulations. The manufacturing of the glasses, the $m = 5$ coating and the assembly was done by SwissNeutronics; The $m = 3.5$ coating was performed at PSI.

A knife edge diaphragm is installed in the centre of the elliptic guide to prevent the direct view in the large divergence setting and to allow for small divergences in cases where off-specular measurements or a clear resolution Δq_z is needed. The blade consists preliminary of a 1 mm BorAl sheet, followed by a 1 mm Cd sheet. It is slightly wider than the guide and it is lead in grooves in the side walls. The diaphragm is motorised and can be varied in the range

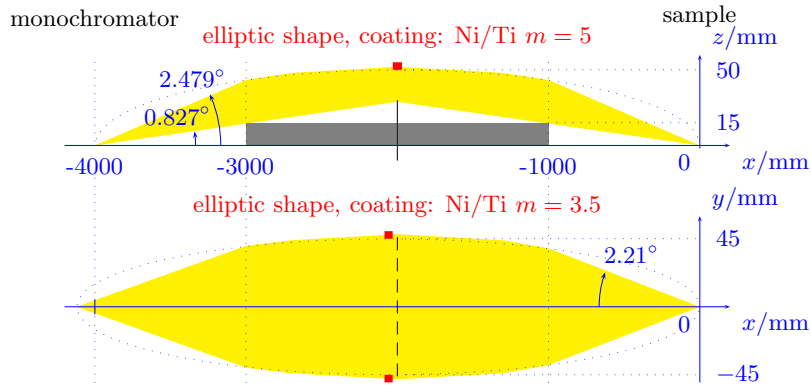


Figure 5: Sketch of the elliptic guide with dimensions. The y and z scales are stretched by a factor 10 relative to the x scale. *Top*: cut in the scattering plane (x - z -plane), *bottom*: cut in the sample plane (x - y -plane).



Figure 6: The guide mounted on the support, with screws to adjust the distance guide to platforms.

0.1 mm to 30 mm, with an accuracy of 0.02 mm.

2.5 sample

For these tests the elliptic guide occupies the sample table. Thus the sample is mounted on the analyser stage. This allows for tilting (θ^s) and lifting (z direction) the sample and thus is sufficient for non-polarised measurements.

For the final set-up intended for Amor the sample will be mounted as in the normal mode on the sample table, allowing for heavy equipment like the 1 T electromagnet, the horizontal 5 T cryomagnet, or the Langmuir trough.

The results shown below were obtained using a Ni film of 1000 Å thickness on glass; and a $m = 5$ Ni/Ti supermirror, also on glass. In addition a perovskite type multilayer and a bi-block-polymer film were used in the monochromatic mode.

2.6 detector

Amor is equipped with 2 ^3He single detectors (diameter 10 mm, active length 100 mm) and a ^3He wire detector with an active window size of $180 \times 180 \text{ mm}^2$. The latter has a spacial resolution of $\approx 2 \text{ mm}$.

3 experiments

A first series of tests of the selene set-up was performed on Amor 2. -6. December 2010.

The set-up and pre-alignment was realised with white light coming from a slight projector and coupled into the neutron beam-path via a Si wafer located between the chopper housing and the 1st slit. The light covers the complete height, but only the inner part in the horizontal plane.

3.1 guide: geometry and alignment

All equipment on the optical bench not needed was removed (i.e. the polariser, slit system 3, sample z -translation). The guide was mounted on an improvised support of X95 profiles, where it was fixed on its centre platform and screws in the end-platforms were used to adjust it (see figure 6). The guide was then aligned with light collimated by slits and by the monochromator. The height and tilting were adjusted to 0 by feeding the beam through openings below the guide, so that the beam and the bottom of the guide were exactly parallel. Then the guide was lowered by 50 mm so that its centre on the upper surface is at the same height as the centre of the monochromator. Afterwards it was tilted by $\theta^e = 1.43^\circ$ to bring the 1st focal point to the position of the initial aperture. In addition the guide was aligned vertically using a narrow light beam.

With the elements located at their nominal posi-

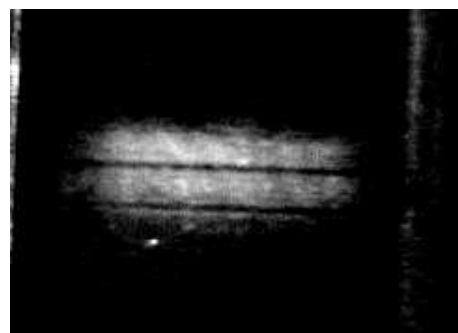


Figure 7: Stripe pattern on the surface of the detector, obtained with white light emerging from the slit at the first focal point. The dark stripes can be related to the glass-glass junction area in the guide.

tions according to figure 8, it was possible to track the light beam to a vertical focal spot some 200 mm upstream from the nominal position. In addition the divergent beam behind the guide showed horizontal stripes which could be associated with the joints of the four 500 mm long individual glass substrates. These stripes can be seen on the detector front in figure 7. The vertical focusing seemed correct with a spot 4000 mm behind the monochromator.

From several tests to improve the guide geometry and form the measurements discussed below it looks like the guide has the following properties:

- The inner parts (along x) of all segments have the correct geometry, both in horizontal and vertical direction. There the waviness and roughness is sufficiently small so it does not affect the working principle.
- In horizontal direction, the 4 segments have a common focal spot, 1010 mm behind the end of the guide. This is sufficiently close to the specified 1000 mm since in horizontal direction the initial aperture is of the order of 20 to 40 mm. Also here one can see dark stripes, but these do not affect the performance of the guide.
- In vertical direction the four segments could not be properly aligned. Segments 1 and 2 can be tuned to share a focal area some 160 mm upstream the nominal position. Dark stripes are still visible since the surface does not follow the elliptic shape close to the ends of the segments. Segments 3 and 4, which produce very sharp spots in their focal distances, are tilted against each other and against the first two. The consequence is that the sample could not be adjusted in a way to ideally be illuminated by all 4 segments. This is the reason for the lower intensity of the reflected beam for higher angles (see figure 12).
- The junction right in the centre of the guide causes the most severe problems. There the surface of the guide seems to be S -shaped with the consequence,

that the neutrons are not just reflected off the sample position. That would just reduce the statistics. But also neutrons from a wrong direction reach the sample, which spoils the $\lambda(\alpha_i)$ encoding. This can be seen *nicely* in figure 10.

In addition the dark region in the centre prevents the operation mode with a small aperture. This would be the fall-back option to the conventional operation, allowing for alignment, and — more severe — for off-specular measurements.

The consequences are, that (I) for these tests the horizontal focusing could not be used; (II) the data collected in the monochromatic mode could not be reduced; and (III) the reference measurement with the guide but a small inner aperture could not be performed. Nevertheless, the principles could be checked and in the case of the TOF mode very good results were obtained, both qualitatively and quantitatively.

3.2 monochromatic mode

The double ML monochromator was mounted on the polariser stage and adjusted with $\theta^m = 0^\circ$ in a way that a collimated beam (defined by the initial slits) just passes through the opening. The knife edge diaphragm is 0.75 mm from the 2nd MLs surface, defining a virtual aperture of 1.5 mm height. Then the monochromator was tilted and shifted to the operation position $\theta^m = 3^\circ$, $z = -7.2$ mm. Accordingly all subsequent components had to be reposition to $z = -7.2$ mm. A sketch of the set-up is shown in figure 8.

The measurements in the monochromatic mode were all done with the chopper running at 700 rpm. Since the slit reducing the beam (the one in the monochromator) was outside of all shielding, the radiation level around the instrument would have been too high other ways.

Figure 9 shows intensity maps obtained from the beam going directly to the detector (no sample), and reflected off of a 1000 Å Ni film on glass, respectively. The black horizontal stripes in the direct measure-

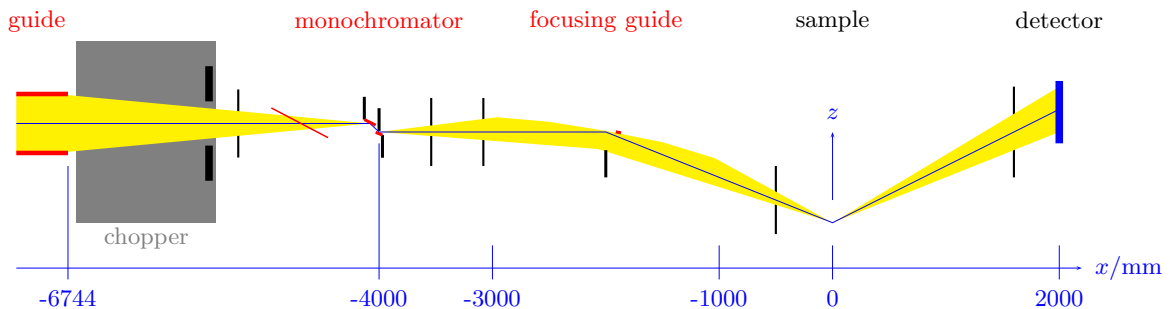


Figure 8: Sketch of Amor in the scattering plane with the test set-up for selene in monochromatic mode. The colour code is: *black*: diaphragms, absorber; *blue*: auxiliary lines and reference beam; *red*: (coated) guide; *yellow*: (part of) beam. The vertical axis is stretched by 10.

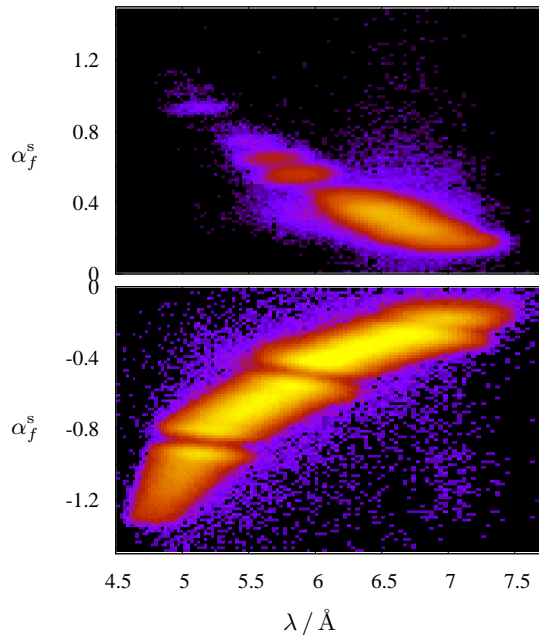


Figure 9: Intensity maps over λ and α_f^s for the 1000 Å Ni film on glass with $\theta^s = 0.5^\circ$ (top), and measured directly by replacing a slit for the sample (bottom).

ments are caused by the junction areas of the elliptic guide not following the nominal curve. Most part of the missing intensity would pass the sample and thus just leads to a reduced statistics. But at least some part of the wrongly scattered intensity makes its way to the sample and thus spoils the $\lambda(\alpha)$ encoding as can be seen in figure 10. The additional stripe pattern for the Ni film measurement in figure 9 is caused by the Kiessig oscillation of the reflectivity and thus the expected signal in this case.

With this set-up several samples were measured with the result that the dynamic range seems to be at least 5 orders of magnitude. The problems with the guide's alignment prevented a proper and quantitative analysis of these measurements.

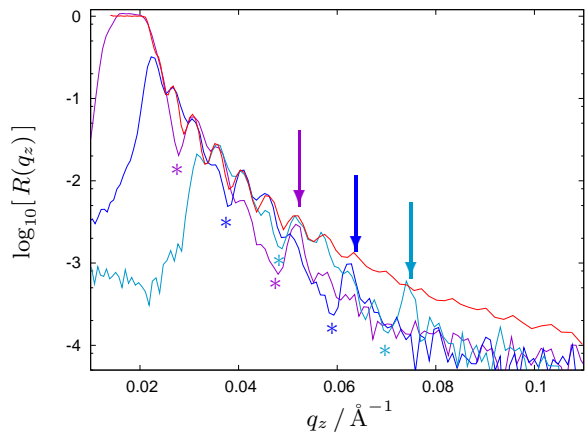


Figure 10: Reflectivity of a 1000 Å Ni film on glass measured in the conventional TOF mode (red) and with the selene set-up in monochromator mode for various θ^s . For the latter the normalisation was not properly performed (the reference measurements are missing) which explains the deviations for larger q_z . But one clearly sees the gaps (marked by asterisks) and pile-ups (marked with arrows) due to the optical errors of the elliptic guide.

3.3 TOF mode

To increase the divergence of the incoming beam to $\approx 1.6^\circ$, the guide was moved closer to the chopper housing (see figure 11). At the 1st focal point a diaphragm is positioned to define the pre-image height of 1 mm. Even with this rather small aperture one had to take care not to oversaturate the area detector, some 8 m away.

Due to the limited time, just the Ni film and the $m = 5$ SM were measured, and only at $\theta^s = 1.25^\circ$ and $\theta^s = 1.75^\circ$. Figure 12 shows one intensity map and the corresponding result of a McStas simulation. The comparison of both shows the effect the misalignment of the real guide: The alignment was optimised for the first segment of the guide, leading to lowest α_i^s . There a good agreement is found with the

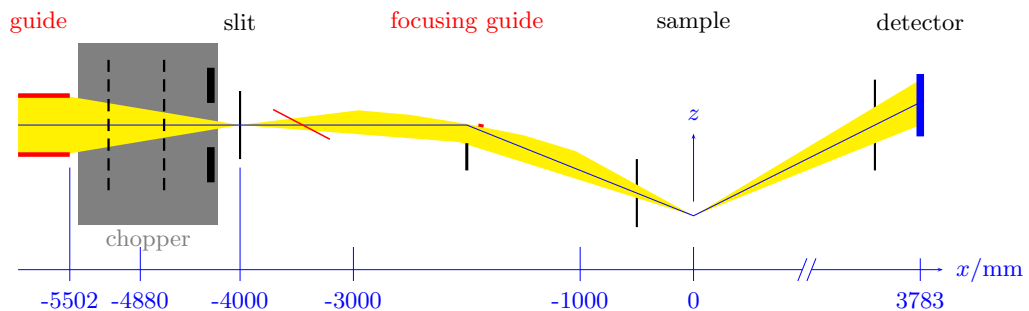


Figure 11: Sketch of Amor in the scattering plane with the test set-up for selene in TOF mode. The colour code is: *black*: diaphragms, absorber; *blue*: auxiliary lines and reference beam; *red*: (coated) guide; *yellow*: (part of) beam. The vertical axis is stretched by 10.

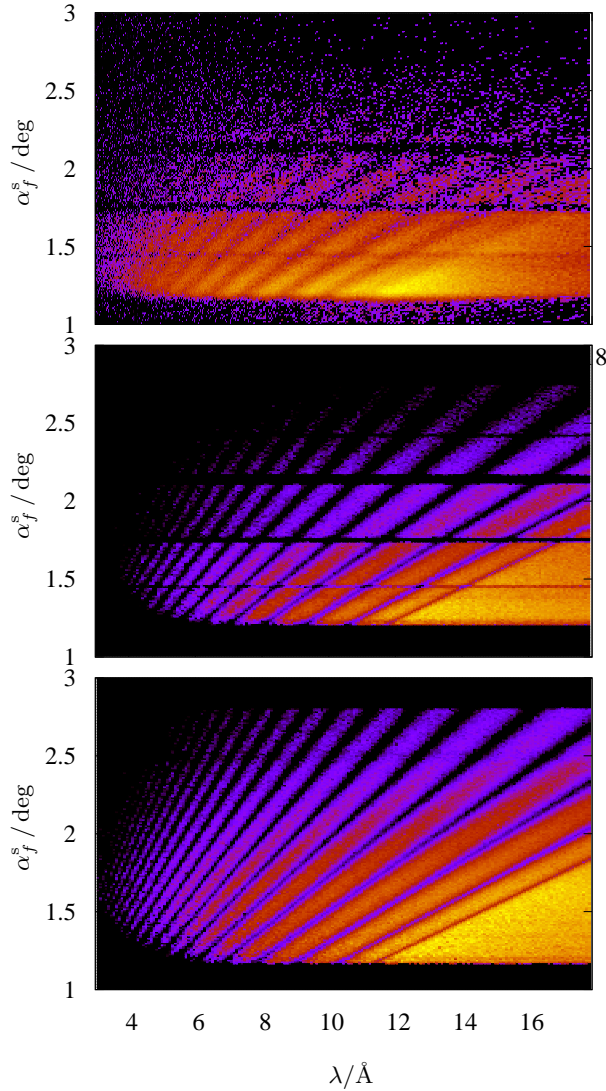


Figure 12: Intensity maps over λ and α_f^s for a 1000 Å Ni film on glass, obtained with a mean angle of incidence $\theta^s = 1.75^\circ$. The intensity is given on \log_{10} scale, where the colour spectrum runs from black ($\log_{10} I = -3$) to yellow ($\log_{10} I = 0$). The *upper* map is as measured and compares to the simulated one in the *middle*. To reproduce the measured intensity distribution in the simulation, the guide segments had to be tilted up to 0.03° relative to each other, shifted in the μm range, and gaps of several cm length were assumed. The *lower* map is also simulated, assuming a perfect alignment and no gaps. The extra horizontal stripes in simulation and measurement (e.g. at $\alpha_f^s \approx 1.3^\circ$ and 2.5°) are caused by features of the straight guide.

simulation. The relative tilt of the other segments leads to a shift of the focal point and thus to reduced intensity and to angular errors.

For the analysis, the λ / α_f^s map was converted to a q_z / α_f^s map pixel by pixel. I.e. every line with constant α_f^s was transformed into a $R(q_z)$ curve.

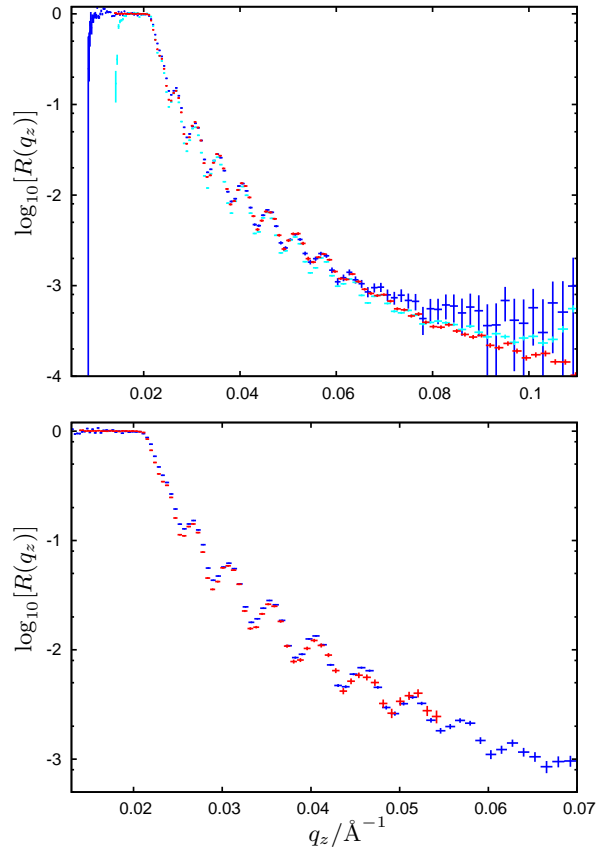


Figure 13: *Top*: $R(q_z)$ for a 1000 Å thick Ni film on glass, obtained from the maps shown in figure 12. The *red* curve is the reference measured in the conventional TOF mode, the *dark blue* and *light blue* curves correspond to $\theta^s = -1.25^\circ$ and $\theta^s = -1.75^\circ$, respectively. *Bottom*: The same $R(q_z)$ curve for $\theta^s = -1.25^\circ$, (*dark blue*), now compared with a single measurement in conventional mode (*red*).

The SM measurements were used for normalising. Subsequently all data points were filled in a new q_z grid with $\Delta q_z / q_z = 0.02$. The resulting $R(q_z)$ curves are shown in figure 13 together with a curve of the same sample, measured in the conventional TOF mode on Amor (with 2 angular settings $\alpha = 0.5^\circ$ and $\alpha = 1.0^\circ$).

The upturn of $R(q_z)$ for large q_z for the selene set-up most likely originate from the fact that the frame-overlap mirror was not used. The reason is that for the selene set-up that one would have to be curved, which is not yet realised. To reduce the influence of frame overlap, the chopper speed was reduced to 700 rpm, i.e. the wavelength range was extended to 26 Å.

The total gain factor for the same resolution is not that easy to extract, since only half the guide worked as expected. The lower graph of figure 13 compares a single conventional measurement (where the parame-

ters on Amor are optimised for) with one using selene. The difference in counting time is a factor 6.7. Taking into account that the chopper speed was reduced from 1500 rpm to 700 rpm (intensity scaled down by 50%) and that the horizontal focusing was missing (another factor 50%) in the second case only, one can estimate a gain factor of ≈ 25 for the same resolution, and at least the same statistics. For higher q_z the gain will be less, since there the incident beam is broader also in the conventional set-up.

4 conclusion

guide

The guide is the weak point of the selene concept. We found that the nominal geometry in the scattering plane was chosen correctly, but that the guide does not fulfil the requirements. At least not for the monochromatic mode and for the high-resolution / off-specular mode with the small aperture.

The 4 individual segments the complete guide is made of have geometrical deviations at the ends, and they are misaligned relative to each other. The consequences are a spoiled $\lambda(\alpha)$ encoding, and dark ranges in α . Away from the ends the shape and surface quality of the guide was fine. So it is most likely a problem of the assembly and adjustment of the individual glass substrates one has to improve.

Normal to the scattering plane the guide works fine.

monochromatic mode

Due to the dark area and the distortions caused by the guide it was not possible to get good reflectivity curves. It was proved that the measurements are feasible, and that gain factors of the order 10 are reachable, but a complete data analysis with comparison to reference measurements has not been done, yet.

TOF mode

Using TOF (for encoding the wavelength) reduced the influence of the shortcomings of the guide dramatically. It was proved that the gain for $q_z < 0.1 \text{ \AA}^{-1}$ is at least one order of magnitude, relative to the conventional set-up — with the same resolution.

the future

Only the very last measurements have been performed with the ideal configuration. So one should repeat the measurements in TOF mode also for more demanding samples and for higher q_z ranges to check the limits of the method. I.e. the influence of off-specular scattering, and the dynamic range reachable.

In addition there are new ideas:

- In TOF mode the measurements were performed with $\theta^s < 0$ i.e. like in the dispersive mode with a ML monochromator. This way the highest intensity is achieved for small λ and small α^s . By tilting the sample to the other side ($\theta^s > 0$) one maps the highest intensity on small λ and large α^s , i.e. on high q_z . At the same time the low resolution (small α^s) corresponds to high q_z and high resolution to small q_z .
- For the remote future a better guide is desirable. For the TOF mode one would gain the horizontal focusing and thus at least a factor 2 in intensity; and the fall-back option to reduce the incoming divergence to conventional values. And the monochromatic mode would be allowed for!
- An option for a new guide is to coat its walls reflecting in the sample plane with polarising supermirrors. This way the *direct* beam would be unpolarised, and the horizontally reflected ones are polarised. With an adequate guide and magnetisation field geometry it should even be possible to magnetise both surfaces in opposite directions, allowing for a simultaneous measurement of both spin states and the unpolarised beam. The 3 signals are horizontally separated on the PSD.

With the presented data we fortify our recommendation to use this concept for new reflectometry beamlines: It allows to start with a tiny aperture, close to the cold source and thus reduces radiation and shielding problems down stream. By using two elliptic guides in series one can avoid aberration and it is possible define the beam at the joining focal point, e.g. by a polariser or a chopper. With the aperture reducing the divergence one has the fall-back option to the conventional TOF or angle dispersive set-up, allowing for off-specular reflectometry.

But also by using the focusing guide element as an add-on for existing instruments one can benefit, as shown by the flux-gain on Amor.

acknowledgments

This research project has been supported – by the European Commission under the 7th Framework Programme through the *Research Infrastructures* action of the *Capacities* Programme, Contract No: CP-CSA-INFRA-2008-1.1.1 Number 226507-NMI3; – by the Swiss National Science Foundation through the *NCCR – Economic stimulus package: Neutron optical devices for small samples*; and – by SwissNeutronics.

For ideas and discussion we thank F. Ott, B. Curbitt, P. Böni, U. Stühr, C. Schanzer, M. Zhernenkov, H. Wacklin, C. Niedermayer, and many others.

References

- [1] Frédéric Ott and Alain Menelle. Refocus: A new concept for a very high flux neutron reflectometer. *Nuclear Instruments and Methods in Physics Research A*, 586(1):23 – 30, 2008. Proceedings of the European Workshop on Neutron Optics - NOP '07.
- [2] J. Stahn, T. Panzner, U. Filges, C. Marcelot, and P. Böni. Study on a focusing, low-background neutron delivery system. *N.I.M. A*, page in press, 2010.
- [3] S. Mühlbauer, P.G. Niklowitz, M. Stadlbauer, R. Georgii, P. Link, J. Stahn, and P. Böni. Elliptic neutron guides—focusing on tiny samples. *Nuclear Instruments and Methods in Physics Research A*, 586(1):77 – 80, 2008. Proceedings of the European Workshop on Neutron Optics - NOP '07.
- [4] S. Mühlbauer, M. Stadlbauer, P. Böni, C. Schanzer, J. Stahn, and U. Filges. Performance of an elliptically tapered neutron guide. *Physica B*, 385-386:1247–1249, 2006.
- [5] Frédéric Ott. Easyref: Energy analysis system for reflectometers. *Nuclear Instruments and Methods in Physics Research A*, 584(2-3):401 – 405, 2008.
- [6] F. Ott and A. Menelle. New designs for high intensity specular neutron reflectometers. *European Physical Journal - Special Topics*, 167:93–99, 2009.
- [7] R. Cubitt. *N.I.M. A*, 558:547–550, 2006.
- [8] P. Böni. New concepts for neutron instrumentation. *N.I.M. A*, 586:1 – 8, 2007.
- [9] M. Gupta, T. Gutberlet, J. Stahn, P. Keller, and D. Clemens. Amor - the time-of-flight neutron reflectometer at SINQ/PSI. *Pramana-Journal of Physics*, 63:57–63, 2004.
- [10] A.A. van Well. Double-disk chopper for neutron time-of-flight experiments. *Physica B: Condensed Matter*, 180-181(2):959 – 961, 1992.
- [11] J. Stahn. A switchable white-beam neutron polariser. *Physica B: Condensed Matter*, 345(1-4):243 – 245, 2004. Proceedings of the Conference on Polarised Neutron and Synchrotron X-rays for Magnetism.